



# OVERFLOW Analysis of the DLR-F11 Configuration from HiLiftPW-2 Including Transition Modeling

**James G. Coder**

*Graduate Assistant/NDSEG Fellow*

*Penn State University*

Presented at the 32<sup>nd</sup> Applied Aerodynamics Conference

AIAA Aviation 2014

Atlanta, GA

June 16-20, 2014



# Outline

- **Background and Motivation**
- Geometry and Case Descriptions
- Solver, Methods, and Grids
- Turbulence and Transition Models
- Selected Results
  - Case 1 (Brackets off)
  - Case 2 (Brackets on)
- Observations, Conclusions, and Future Work



## Background

- First AIAA High-Lift Prediction Workshop (HiLiftPW-1) held June, 2010 in Chicago
  - Focused on NASA/Boeing Trapezoidal Wing (Trap Wing)
  - One Reynolds number, two flap deflections
  - Typical industrial CFD analyses agreed well with experiment
  - Best agreement was attained when slat/flap brackets were not modeled
- Special Session held June, 2012 in New Orleans
  - Extended analysis of HiLiftPW-1 cases
  - Laminar-turbulent transition improved brackets-on predictions
- HiLiftPW-2 held June, 2013 in San Diego
  - Following the success of HiLiftPW-1
  - New configuration, DLR-F11, representative of commercial transports
  - Two Reynolds numbers, one flap deflection



## Motivation

- Did not participate in HiLiftPW-1 or the follow-up Special Session
- High lift analysis capabilities
  - Refine workflow for complex configurations
  - Validate approach to solution (methods, models, etc.)
- Transition modeling
  - Transition modeling had a huge impact on HiLiftPW-1
  - New CFD-compatible transition model developed for PhD dissertation
- Identify modeling deficiencies
  - Which turbulence model performs best and why?
  - Is steady RANS sufficient for high-lift flows?



# Outline

- Background and Motivation
- **Geometry and Case Descriptions**
- Solver, Methods, and Grids
- Turbulence and Transition Models
- Selected Results
  - Case 1 (Brackets off)
  - Case 2 (Brackets on)
- Observations, Conclusions, and Future Work

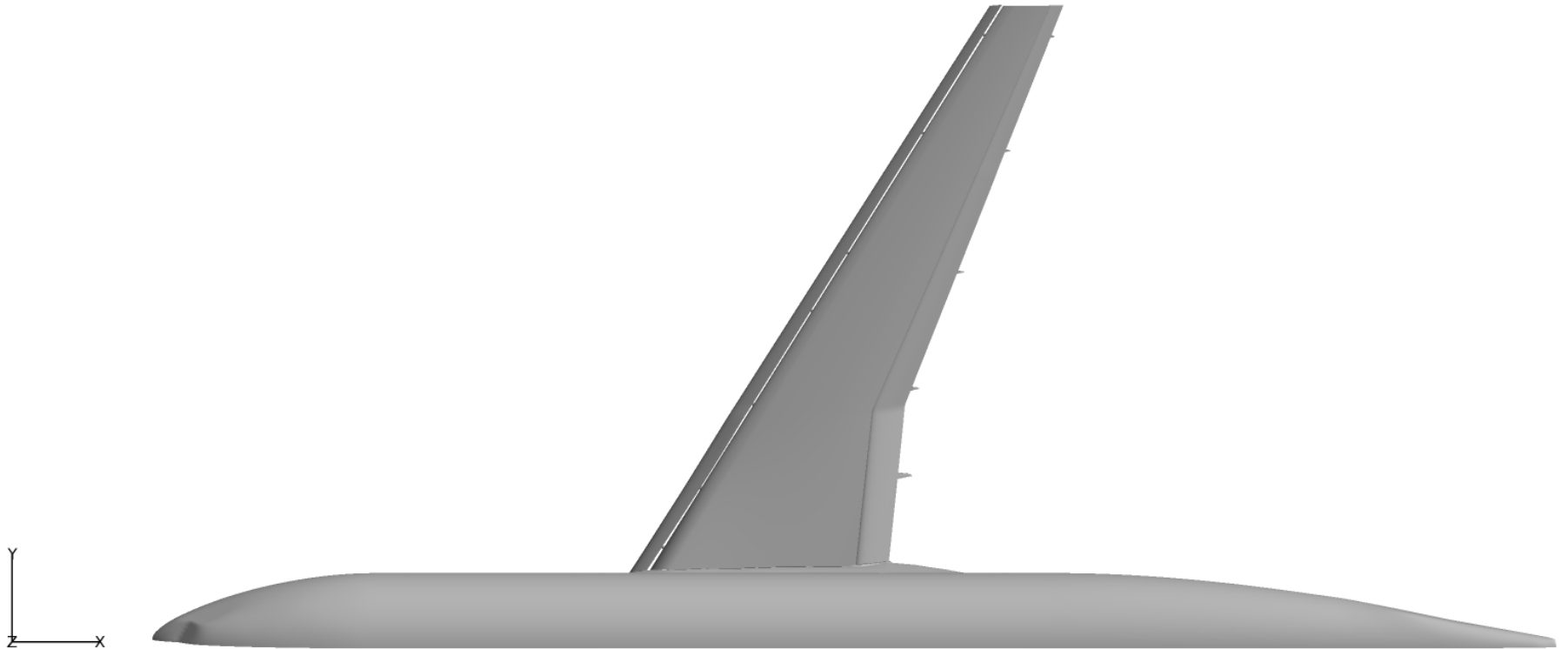


- DLR F11 (wind-tunnel model)





- DLR F11 (computational model)





## Case Descriptions

- Case 1 – Grid convergence study (Config. 2)
  - $M = 0.175$
  - $Re = 15.1 \times 10^6$
  - $T_{ref} = 205.2 \text{ R}$
  - Angles of attack (deg): 7, 16, 18.5, 20, 21, 22.4, [24, 25, 26, 27, 28]
- Case 2a – Low-Reynolds Number Condition (Config. 4)
  - $M = 0.175$
  - $Re = 1.35 \times 10^6$
  - $T_{ref} = 537.48 \text{ R}$
  - Angles of attack (deg): 0, 7, 12, 16, 18.5, 19, 20, 21



## Case Descriptions

- Case 2b – High-Reynolds Number Condition (Config. 4)
  - $M = 0.175$
  - $Re = 15.1 \times 10^6$
  - $T_{ref} = 205.2 \text{ R}$
  - Angles of attack (deg): 0, 7, 12, 16, 18.5, 20, 21, 22.4
- Case 2c – Low-Reynolds Number Condition with Transition (Config. 4)
  - Optional Study
  - $M = 0.175$
  - $Re = 1.35 \times 10^6$
  - $T_{ref} = 537.48 \text{ R}$
  - Angles of attack (deg): 0, 7, 12, 16, 18.5, 19, 20, 21



## Case Descriptions

- Case 3 – Full Configuration Study (Config. 5)
  - Optional study
  - Cases 3a and 3b same as 2a and 2b, but using Config. 5
  - NOT ANALYZED
- Case 4 – Turbulence Model Grid-Convergence Verification Study
  - Optional but highly encouraged study
  - Uses the 2-D bump-in-channel geometry from NASA Turbulence Modeling Resource
  - Included in paper (AIAA 2014-2696)



## Outline

- Background and Motivation
- Geometry and Case Descriptions
- **Solver, Methods, and Grids**
- Turbulence and Transition Models
- Selected Results
  - Case 1 (Brackets off)
  - Case 2 (Brackets on)
- Observations, Conclusions, and Future Work



## Solver and Methods

- OVERFLOW 2.2f
  - Maintained by NASA
  - Structured, overset solver
  - Variety of discretization schemes and implicit algorithms
  - Several turbulence models, and now transition ( $\gamma$ - $Re_{\theta t}$ )
- Methods for HiLiftPW-2
  - Committee-provided overset grid system
  - 3<sup>rd</sup>-order Roe scheme
  - Non-time-accurate scalar pentadiagonal implicit algorithm
  - Spalart-Allmaras (1-equation) and Menter SST (2-equation) turbulence models
  - Coder-Maughmer (1-equation, custom implementation) and Langtry-Menter (2-equation) transition models
  - Rotation/curvature correction (Spalart-Shur)
  - Low-Mach preconditioning



## Overset Grid System

- Generated by Sclafani et al., Boeing - Huntington Beach
- Config. 2 (Case 1, brackets off), 44 grids
  - Coarse: 29,386,628 grid points
  - Medium: 69,014,980 grid points
  - Fine: 230,770,520 grid points
  - Extra-fine: 544,468,508 grid points – NOT ANALYZED
- Config. 4 (Case 2, Config. 2 + brackets), 163 grids
  - Medium: 97,200,442 grid points
- Config. 5 (Case 3, Config. 4 + pressure tube bundles), 190 grids
  - Medium: 100,748,677 grid points – NOT ANALYZED



## Outline

- Background and Motivation
- Geometry and Case Descriptions
- Solver, Methods, and Grids
- **Turbulence and Transition Models**
- Selected Results
  - Case 1 (Brackets off)
  - Case 2 (Brackets on)
- Observations, Conclusions, and Future Work



# Turbulence Models

- Spalart-Allmaras (SA)

$$\frac{\partial \tilde{\nu}}{\partial t} + u_j \frac{\partial \tilde{\nu}}{\partial x_j} = c_{b1} \tilde{S} \tilde{\nu} (1 - f_{t2}) - \left[ c_{w1} f_w - \frac{c_{b1}}{\kappa^2} \right] \left( \frac{\tilde{\nu}}{d} \right)^2 + \frac{1}{\sigma} \left[ \frac{\partial}{\partial x_j} \left( (\nu + \tilde{\nu}) \frac{\partial \tilde{\nu}}{\partial x_j} \right) + c_{b2} \frac{\partial \tilde{\nu}}{\partial x_j} \frac{\partial \tilde{\nu}}{\partial x_j} \right]$$

$$\mu_t = \rho \frac{\tilde{\nu}^4}{\tilde{\nu}^3 + (c_{v1} \nu)^3}$$

- Widely used in external aerodynamics
- Successful in Drag Prediction Workshop series and HiLiftPW-1
- Fully turbulent version in OVERFLOW omits  $f_{t2}$  terms (SA-noft2)



# Turbulence Models

- Menter Shear Stress Transport (SST)

$$\frac{\partial(\rho k)}{\partial t} + \frac{\partial(\rho u_j k)}{\partial x_j} = \mu_t S^2 - \beta^* \rho k \omega + \frac{\partial}{\partial x_j} \left[ \left( \mu + \frac{\mu_t}{\sigma_k} \right) \frac{\partial k}{\partial x_j} \right]$$

$$\frac{\partial(\rho \omega)}{\partial t} + \frac{\partial(\rho u_j \omega)}{\partial x_j} = \alpha S^2 - \beta \rho \omega^2 + \frac{\partial}{\partial x_j} \left[ \left( \mu + \frac{\mu_t}{\sigma_\omega} \right) \frac{\partial \omega}{\partial x_j} \right] + 2(1 - F_1) \frac{\rho \sigma_{\omega 2}}{\omega} \frac{\partial k}{\partial x_j} \frac{\partial \omega}{\partial x_j}$$

$$\mu_t = \frac{\rho a_1 k}{\max(a_1 \omega, \Omega F_2)}$$

- Very popular for industrial aerodynamic applications
- Constants and cross-diffusion term blended between  $k$ - $\omega$  behavior (near wall) and  $k$ - $\epsilon$  behavior (free-stream and outer boundary layer)



# Transition Models

- Coder-Maughmer Amplification Factor Transport (AFT)

$$\frac{\partial(\rho\tilde{n})}{\partial t} + \frac{\partial(\rho u_j \tilde{n})}{\partial x_j} = \rho \Omega F_{crit} F_{growth} \frac{d\tilde{n}}{dR_{\delta 2}} + \frac{\partial}{\partial x_j} \left[ \left( \mu + \frac{\mu_t}{\sigma_n} \right) \frac{\partial \tilde{n}}{\partial x_j} \right]$$

- CFD-compatible model of approximate envelope  $e^N$  method
- Uses a local shape factor to estimate integral boundary layer properties

$$H_{12} = f \left( \frac{Sd}{U_e} \right)$$

- Currently applied to Spalart-Allmaras model through modification of  $f_{t2}$  function
- SST implementation under development



# Transition Models

- Langtry-Menter  $\gamma-Re_{\theta t}$  (LM)

$$\frac{\partial(\rho\gamma)}{\partial t} + \frac{\partial(\rho u_j \gamma)}{\partial x_j} = F_{length} c_{a1} \rho S [\gamma F_{onset}]^{0.5} (1 - c_{e1} \gamma)$$

$$-c_{a2} \rho \Omega \gamma F_{turb} (c_{e2} \gamma - 1) + \frac{\partial}{\partial x_j} \left[ \left( \mu + \frac{\mu_t}{\sigma_f} \right) \frac{\partial \gamma}{\partial x_j} \right]$$

$$\frac{\partial(\rho \overline{Re_{\theta t}})}{\partial t} + \frac{\partial(\rho u_j \overline{Re_{\theta t}})}{\partial x_j} = c_{\theta t} \frac{\rho}{t} (Re_{\theta t} - \overline{Re_{\theta t}}) (1 - F_{\theta t}) + \frac{\partial}{\partial x_j} \left[ \sigma_{\theta t} (\mu + \mu_t) \frac{\partial \overline{Re_{\theta t}}}{\partial x_j} \right]$$

- CFD-compatible model of local correlation transition method
- Applied to Menter SST turbulence model where effective intermittency multiplies turbulent kinetic energy source terms



## Turbulence/Transition Model Applications

- Case 1
  - SA-noft2
  - SA-noft2-RC (medium grid only)
- Case 2, High Re
  - SA-noft2
  - SA-noft2-RC
- Case 2, Low Re
  - SA-noft2
  - SA-noft2-RC
  - SST
  - SA-AFT
  - SA-RC-AFT
  - SA-QCR2000-AFT
  - SST-LM
  - SST-QCR2000-LM

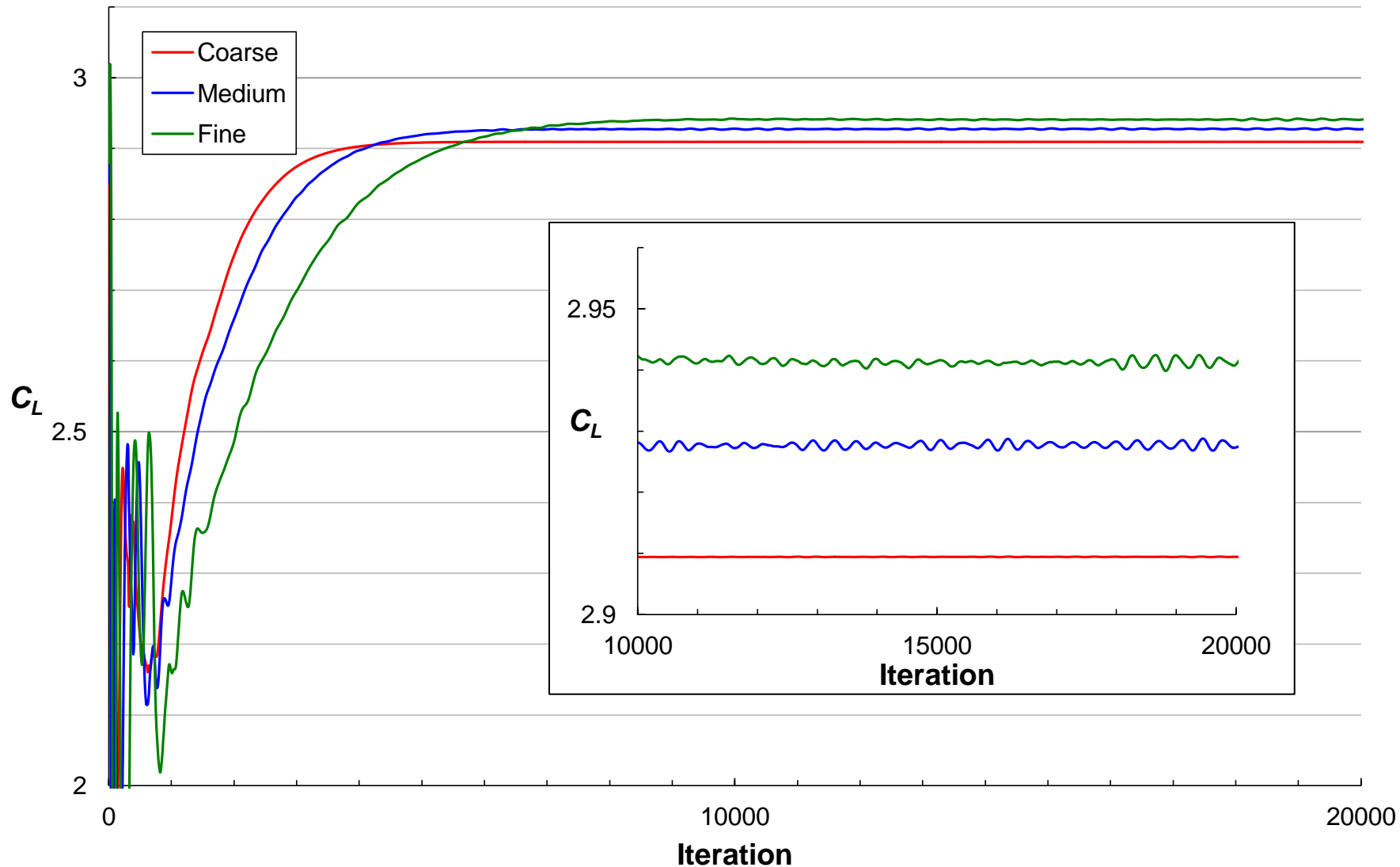


## Outline

- Background and Motivation
- Geometry and Case Descriptions
- Solver, Methods, and Grids
- Turbulence and Transition Models
- **Selected Results**
  - **Case 1 (Brackets off)**
  - Case 2 (Brackets on)
- Observations, Conclusions, and Future Work



# Typical Force/Moment Convergence Behavior

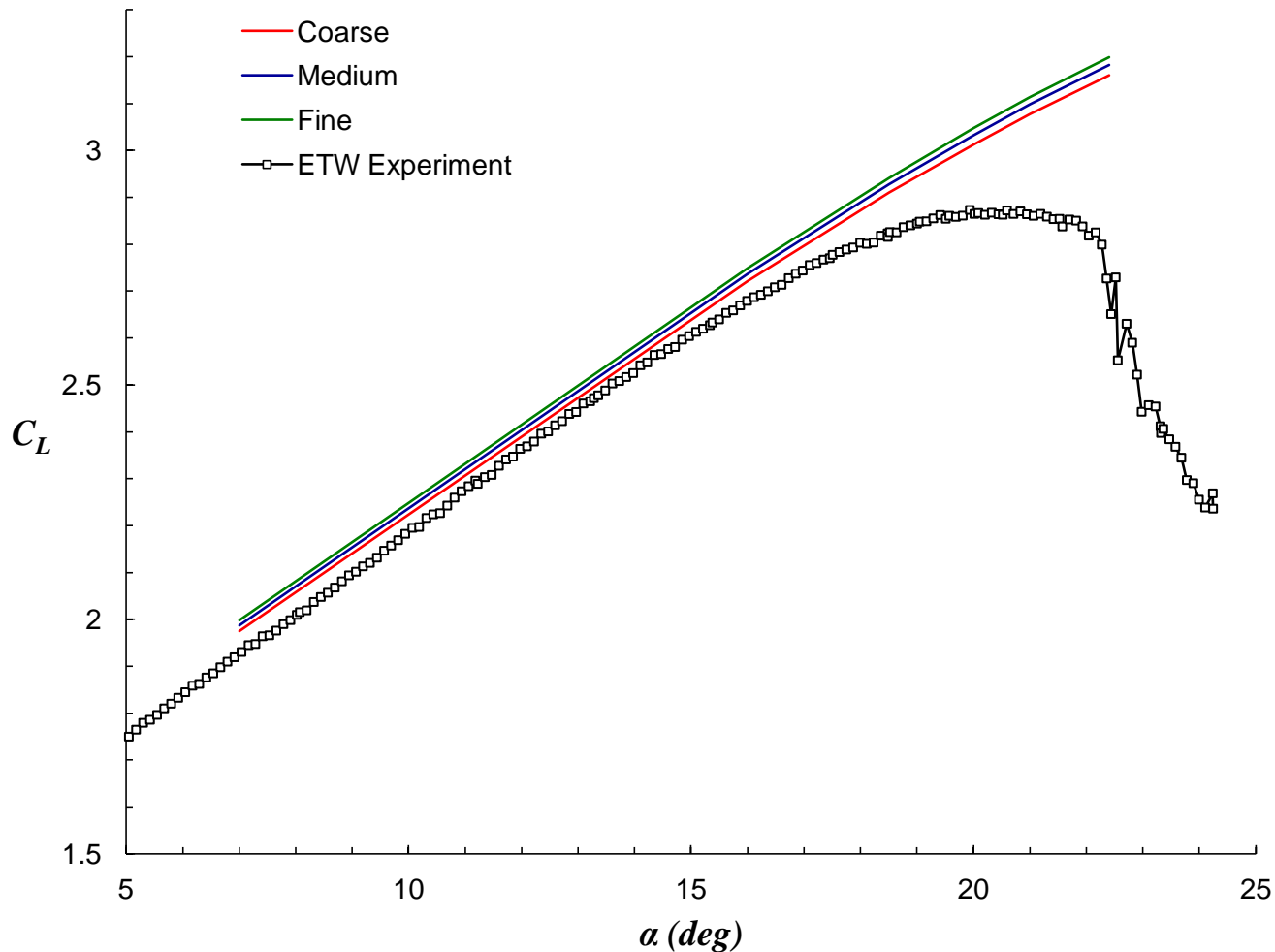




Case 1

Grid Convergence Study,  $Re = 15.1 \times 10^6$

- Lift, SA-noft2

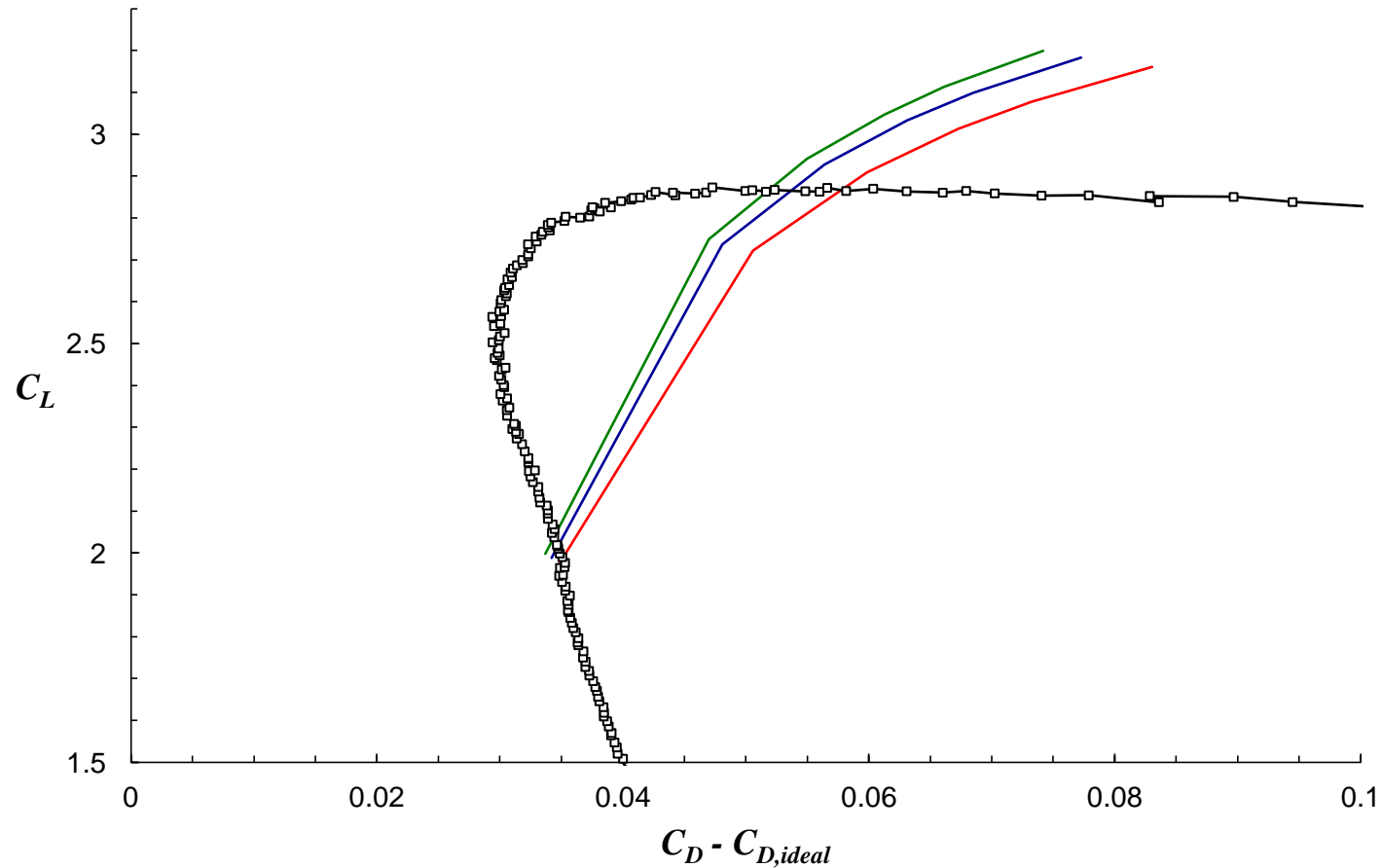




Case 1

Grid Convergence Study,  $Re = 15.1 \times 10^6$

- “Profile” Drag, SA-noft2

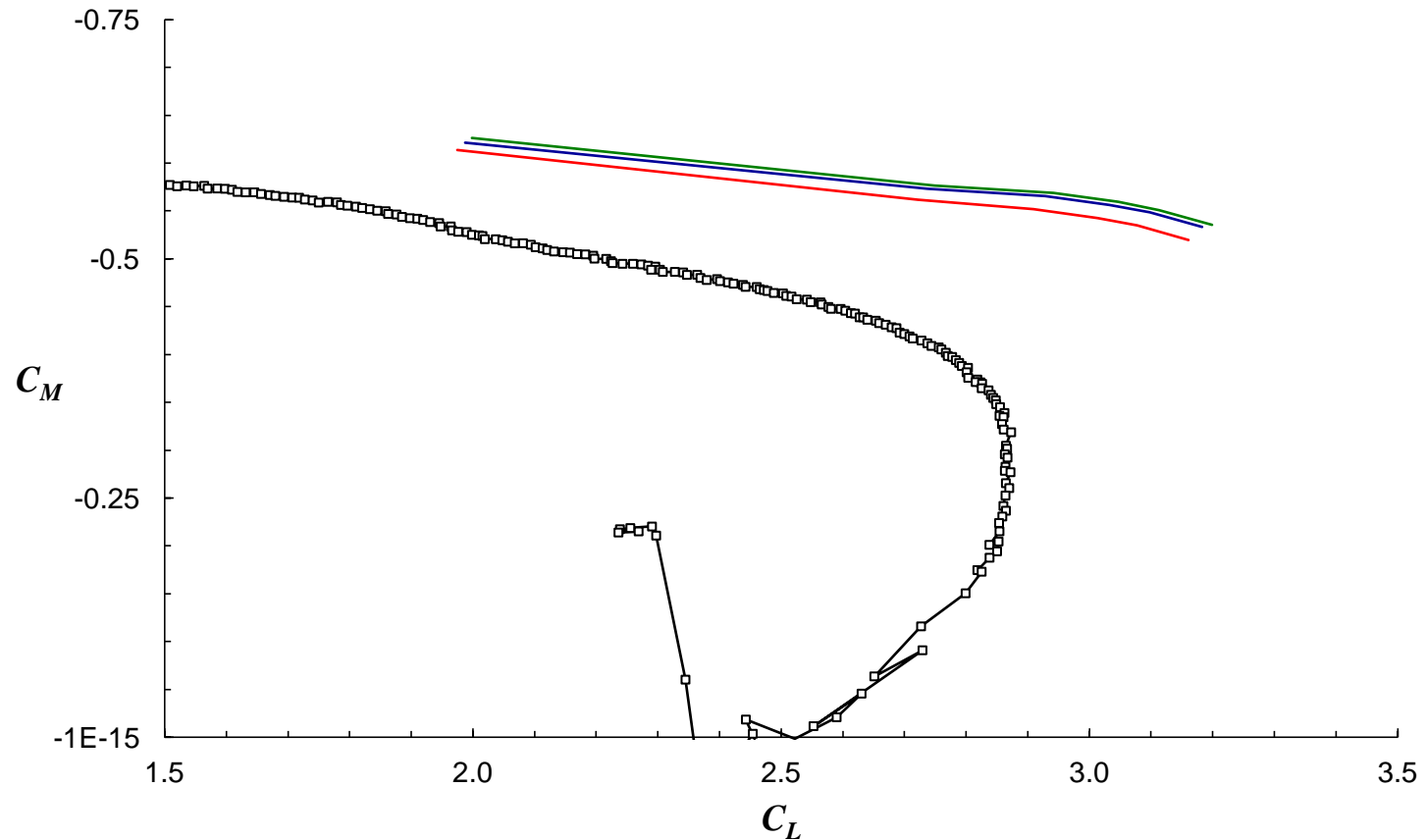




Case 1

Grid Convergence Study,  $Re = 15.1 \times 10^6$

- Pitching Moment, SA-noft2

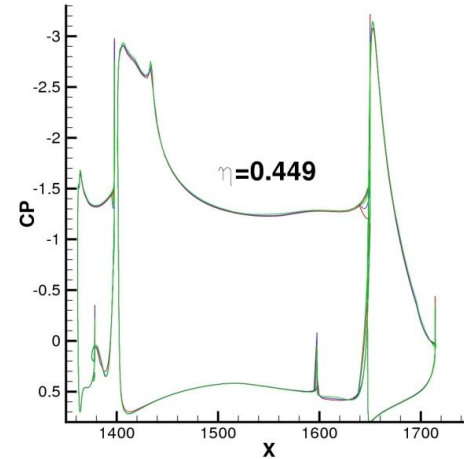
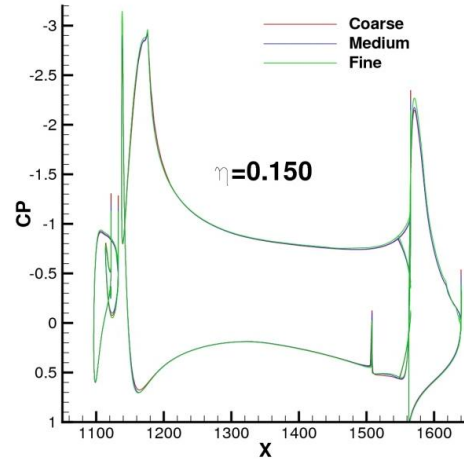




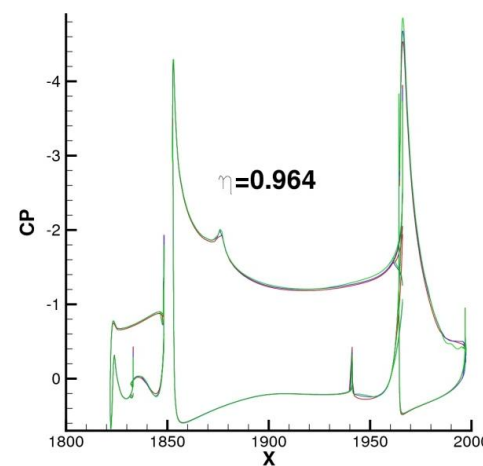
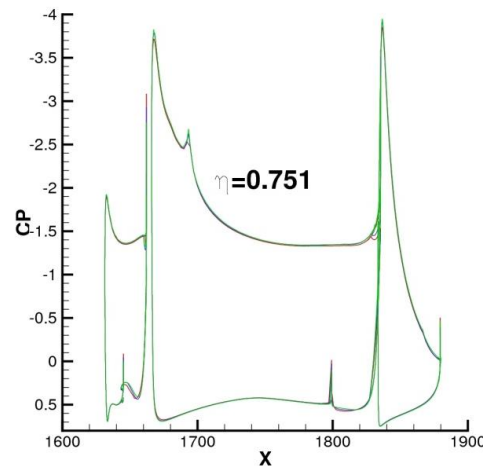
Case 1

Grid Convergence Study,  $Re = 15.1 \times 10^6$

- Pressure distributions, SA-noft2,  $\alpha = 7^\circ$



$\alpha = 7^\circ$

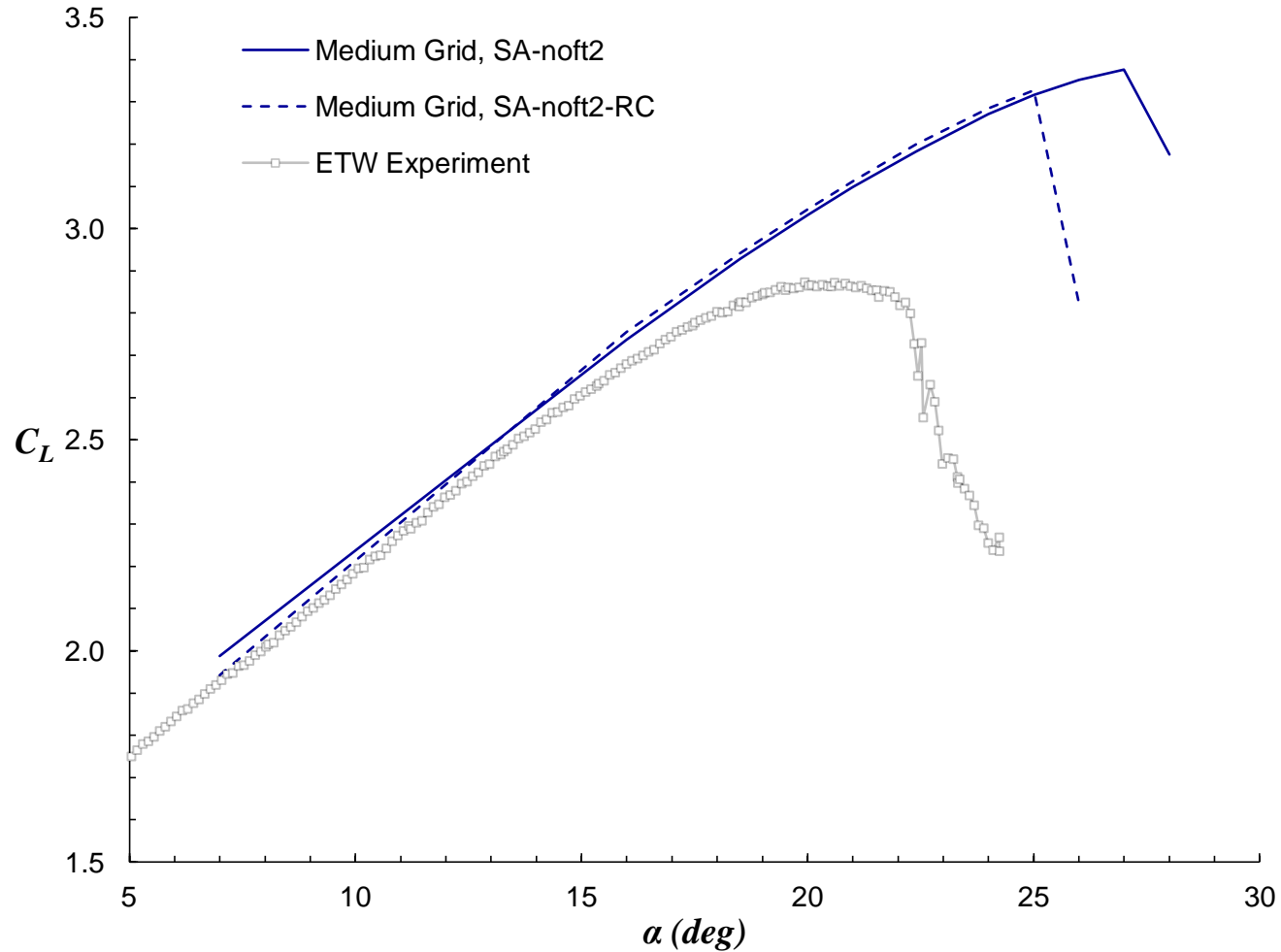




Case 1

Effect of RC Correction,  $Re = 15.1 \times 10^6$

- Lift

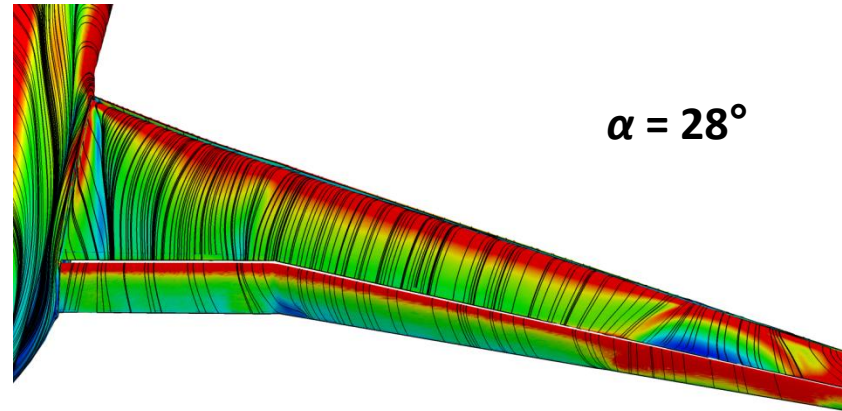




**Case 1**

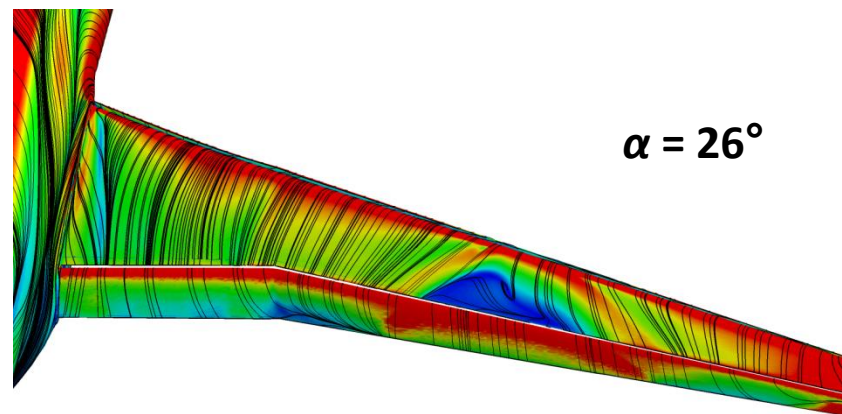
Effect of RC Correction,  $Re = 15.1 \times 10^6$

- Surface flow patterns (vorticity)



$\alpha = 28^\circ$

SA-noft2



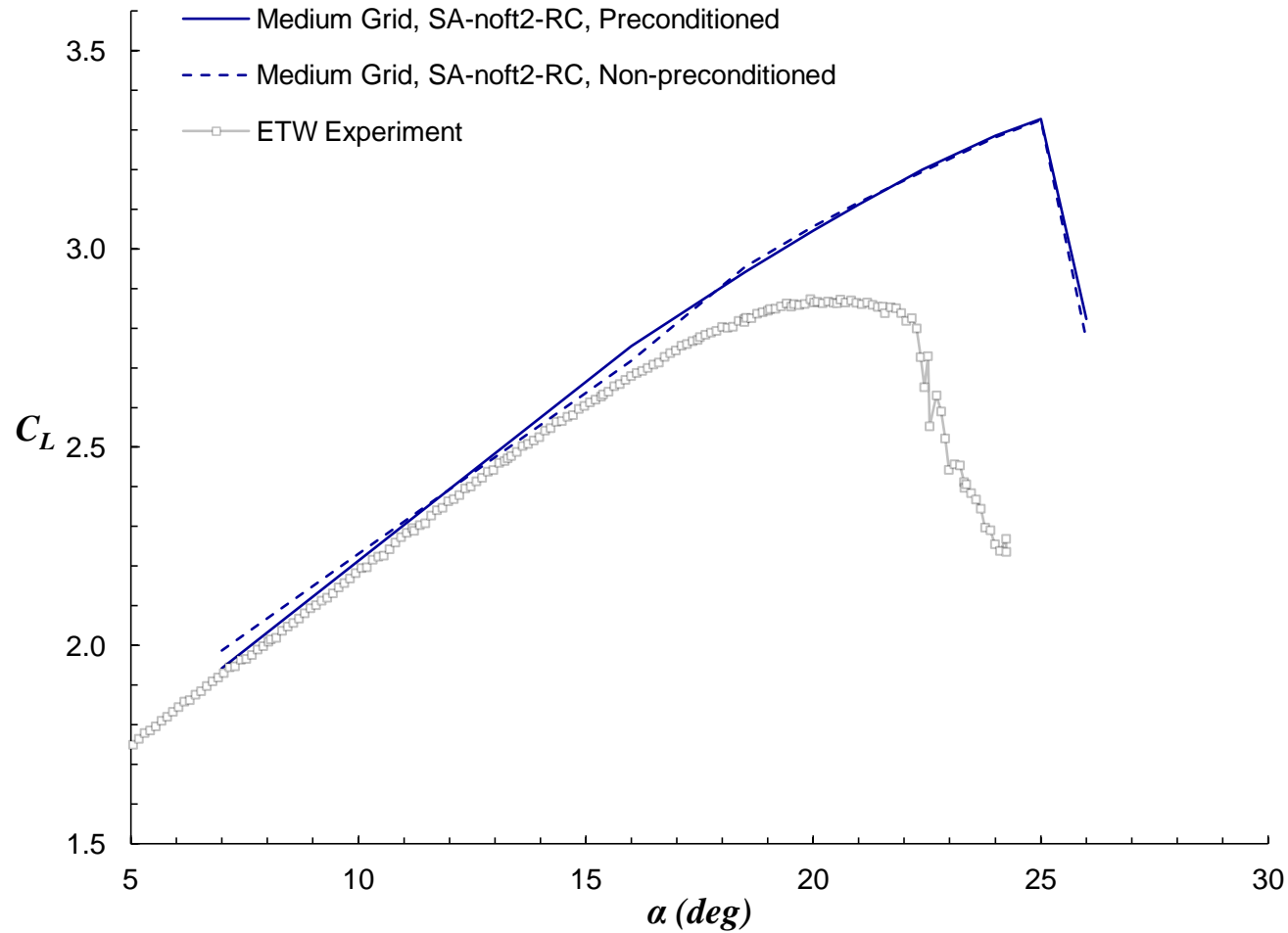
$\alpha = 26^\circ$

SA-noft2-RC



# Effect of Low-Mach Preconditioning, $Re = 15.1 \times 10^6$

- Lift

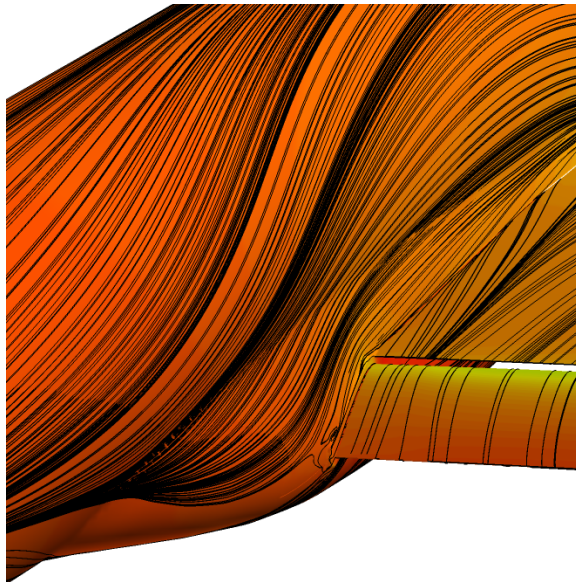




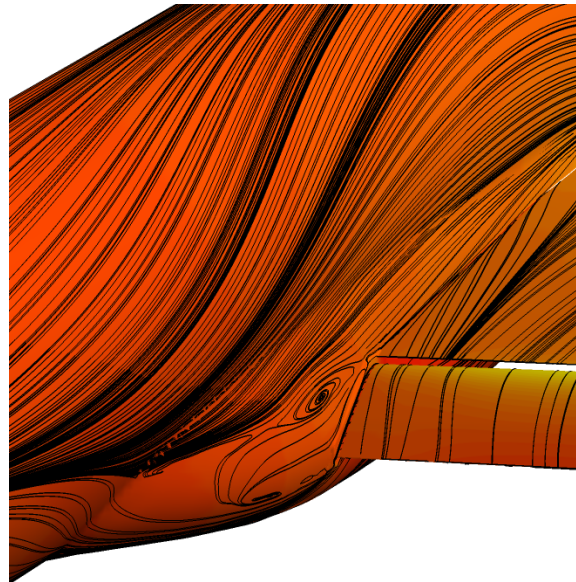
Case 1

Effect of Low-Mach Preconditioning,  $Re = 15.1 \times 10^6$

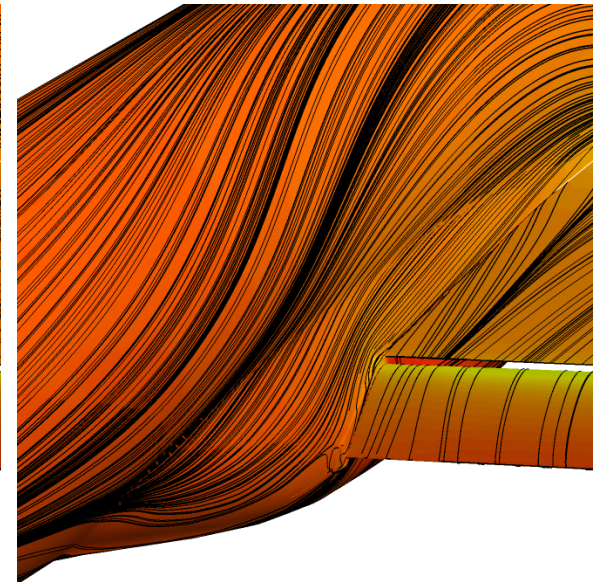
- Surface flow patterns (pressure),  $\alpha = 7^\circ$



**SA-noft2  
Preconditioned**



**SA-noft2-RC  
Preconditioned**



**SA-noft2-RC  
Not preconditioned**



## Outline

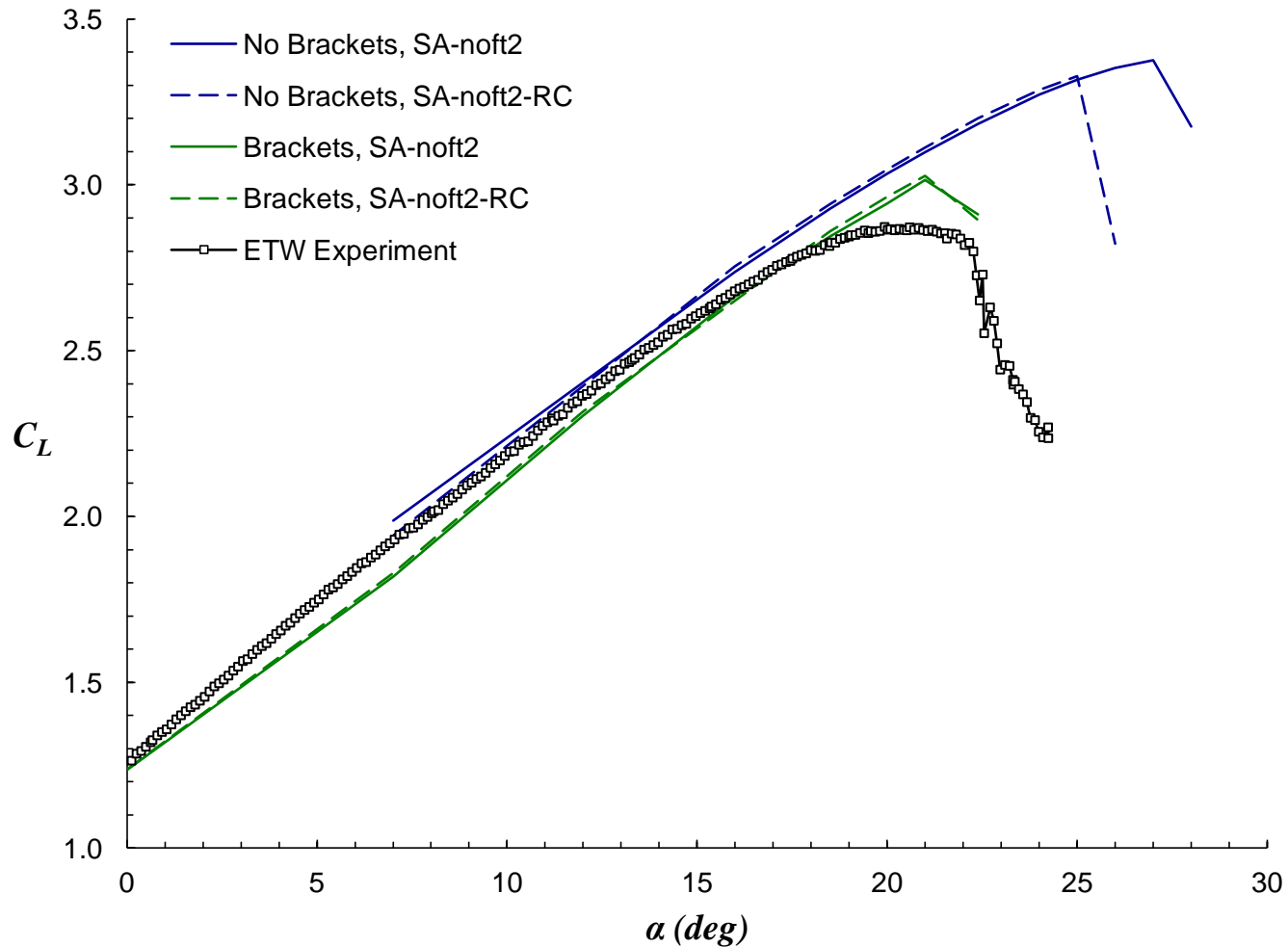
- Background and Motivation
- Geometry and Case Descriptions
- Solver, Methods, and Grids
- Turbulence and Transition Models
- **Selected Results**
  - Case 1 (Brackets off)
  - **Case 2 (Brackets on)**
- Observations, Conclusions, and Future Work



Case 2

Effect of Slat and Flap Brackets,  $Re = 15.1 \times 10^6$

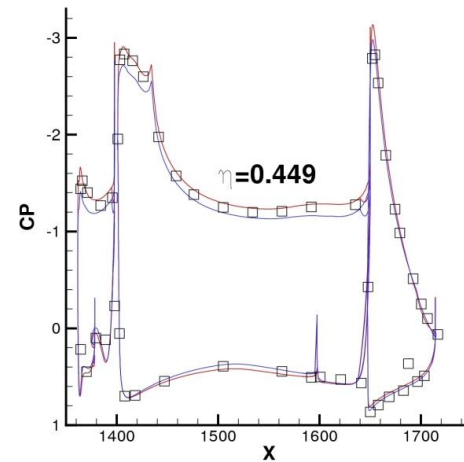
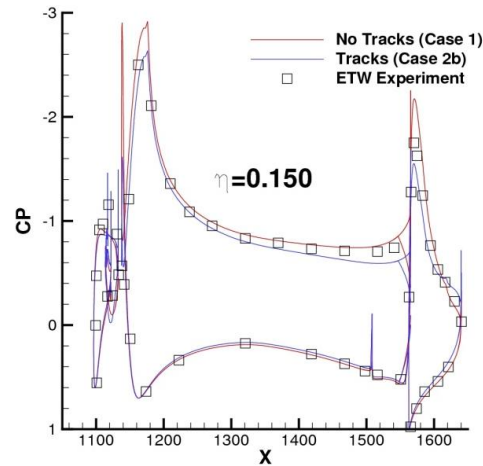
- Lift



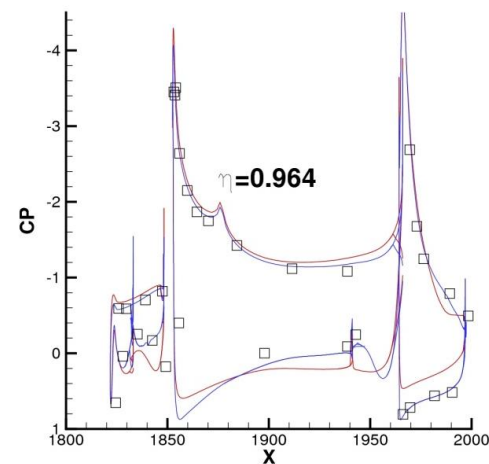
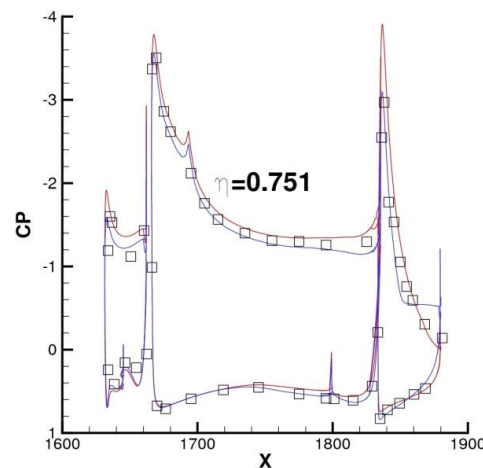


# Effect of Slat and Flap Brackets, $Re = 15.1 \times 10^6$

- Pressure distributions,  $\alpha = 7^\circ$



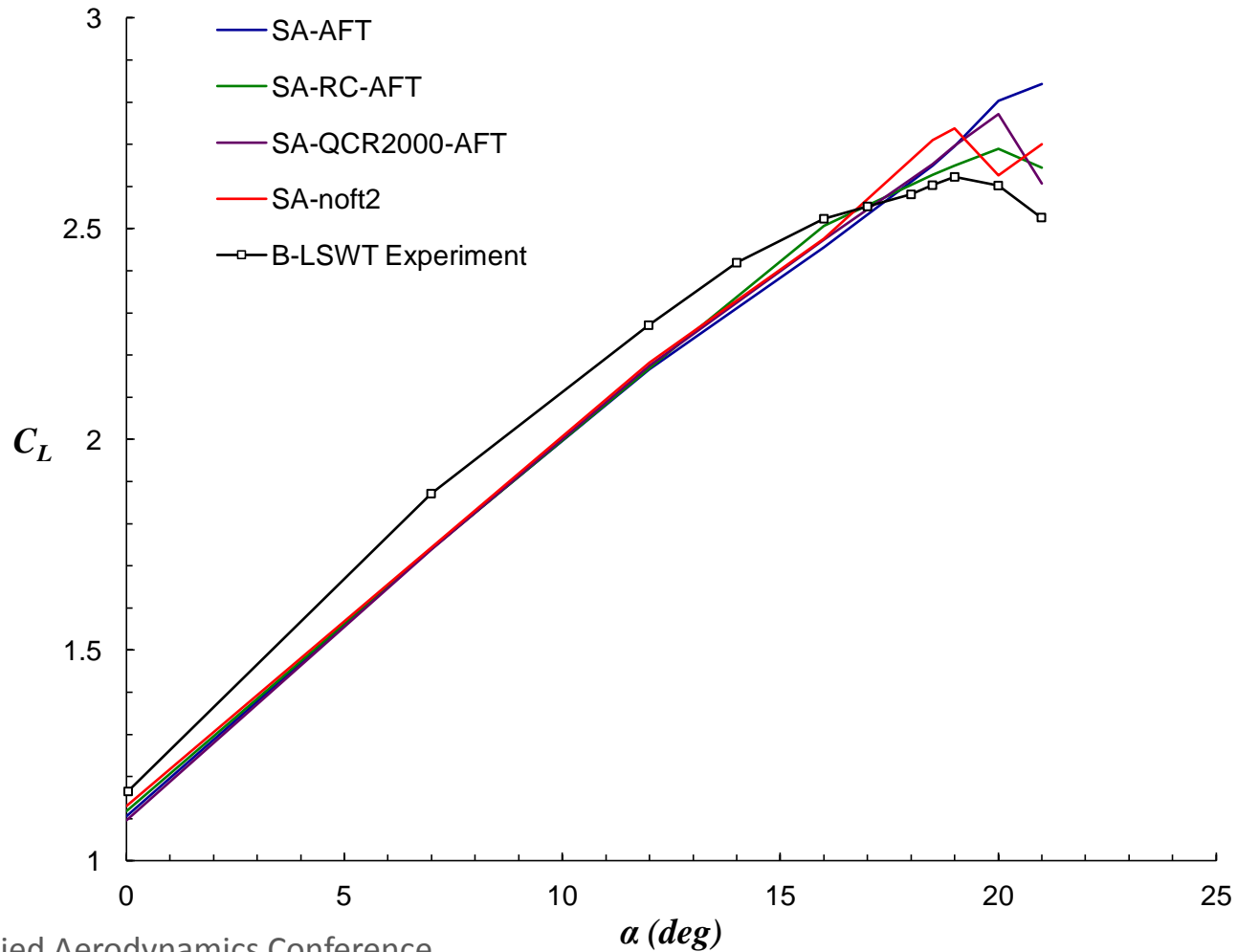
$\alpha = 7^\circ$





# Effect of Transition Modeling, $Re = 1.35 \times 10^6$

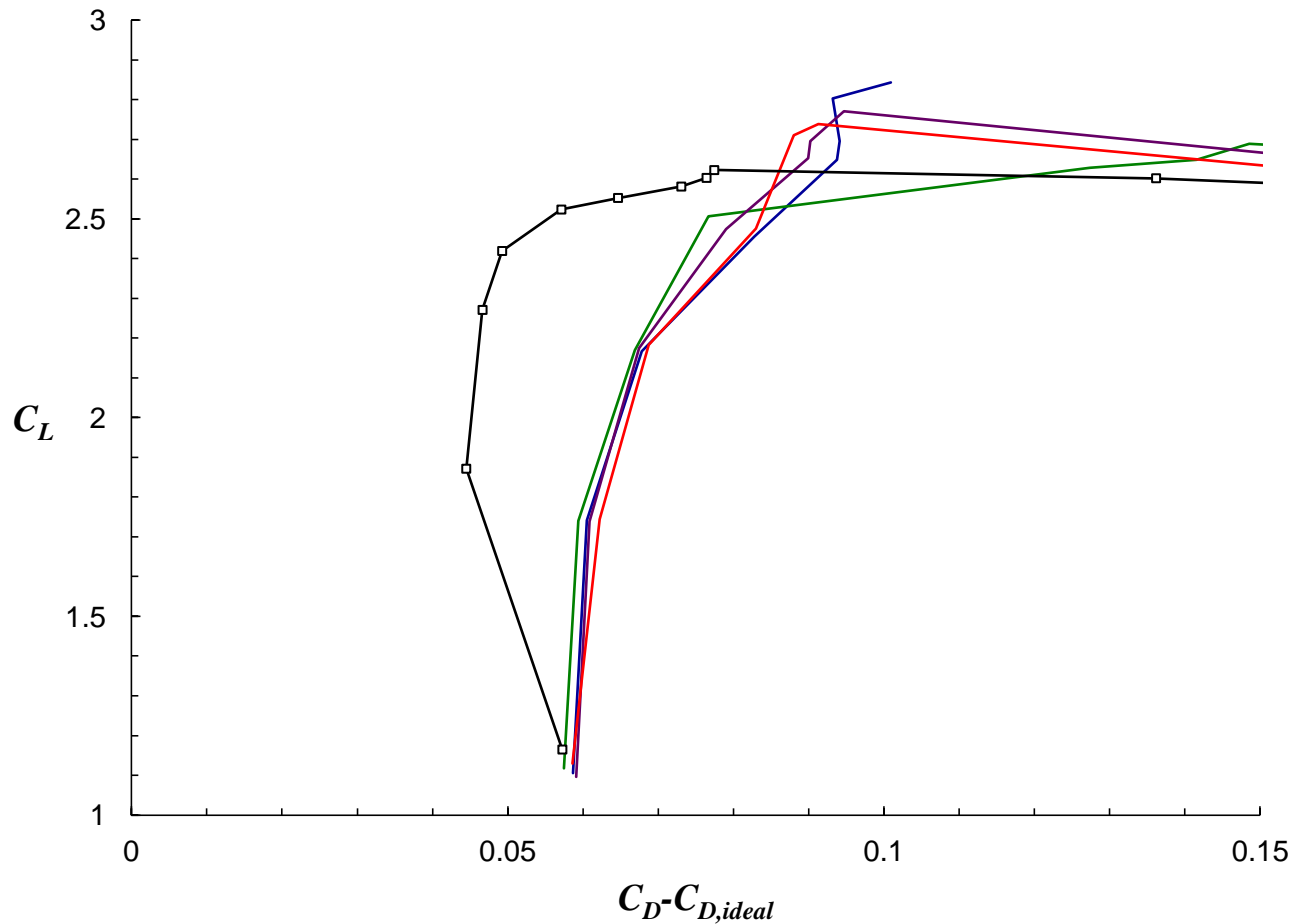
- Lift, SA-based models





# Effect of Transition Modeling, $Re = 1.35 \times 10^6$

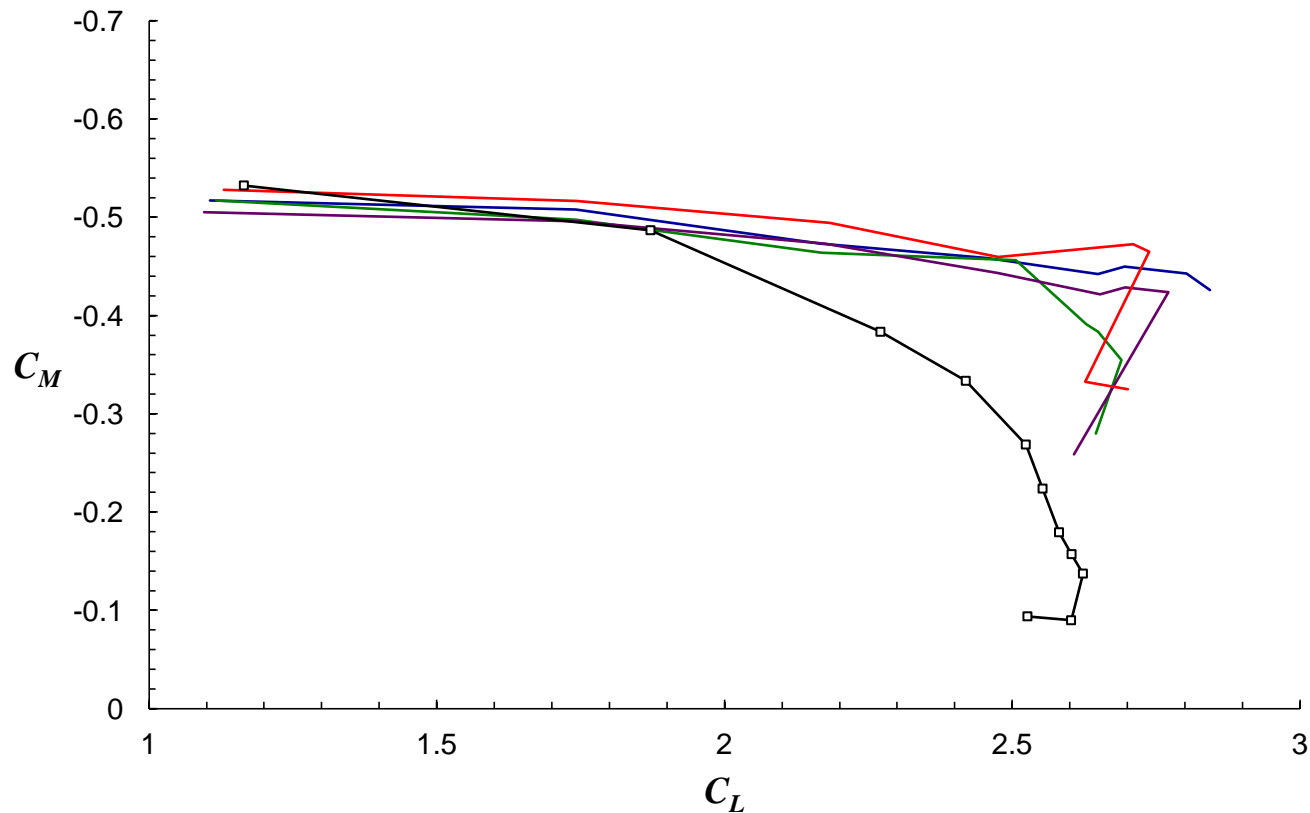
- “Profile” Drag, SA-based models





# Effect of Transition Modeling, $Re = 1.35 \times 10^6$

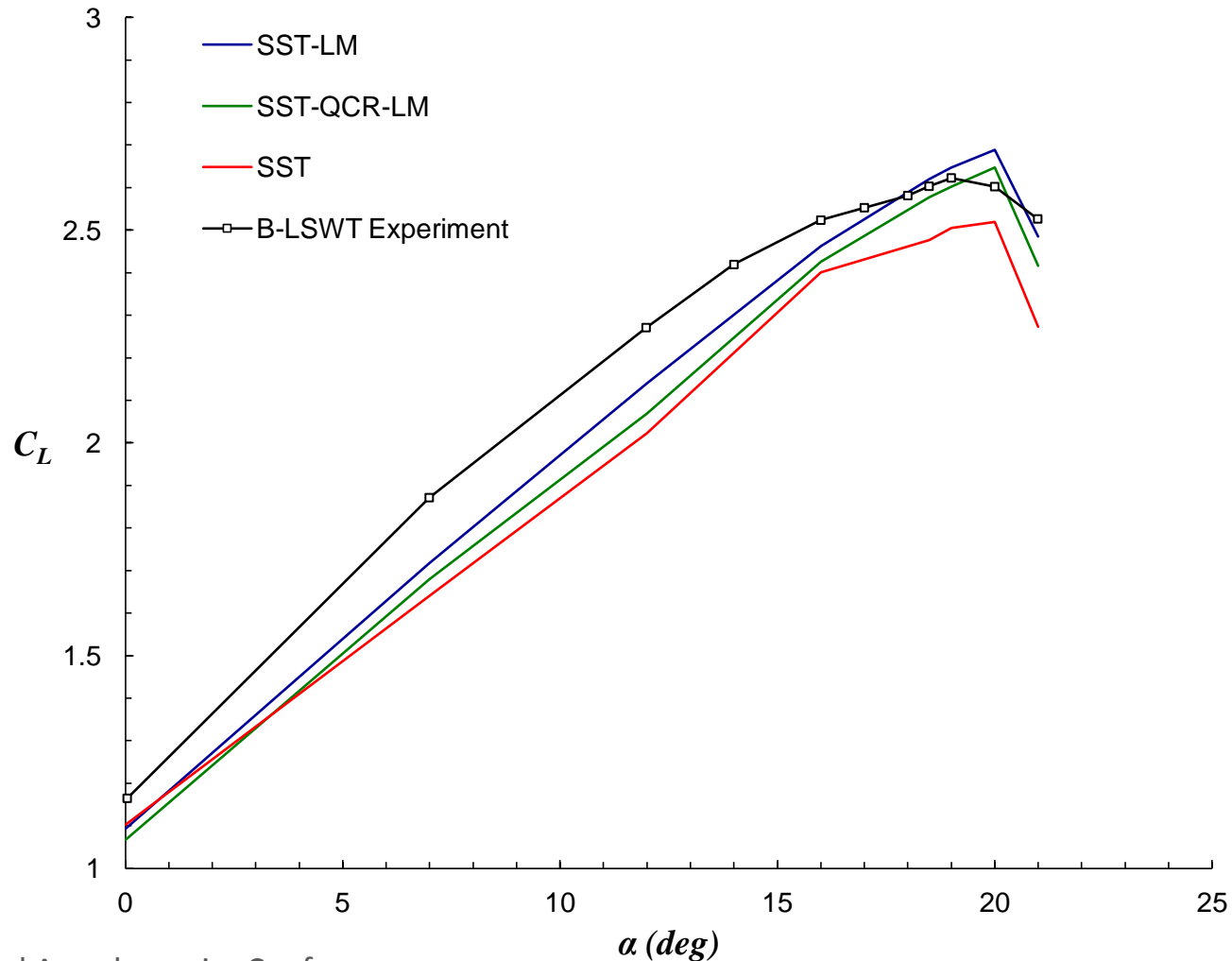
- Pitching Moment, SA-based models





# Effect of Transition Modeling, $Re = 1.35 \times 10^6$

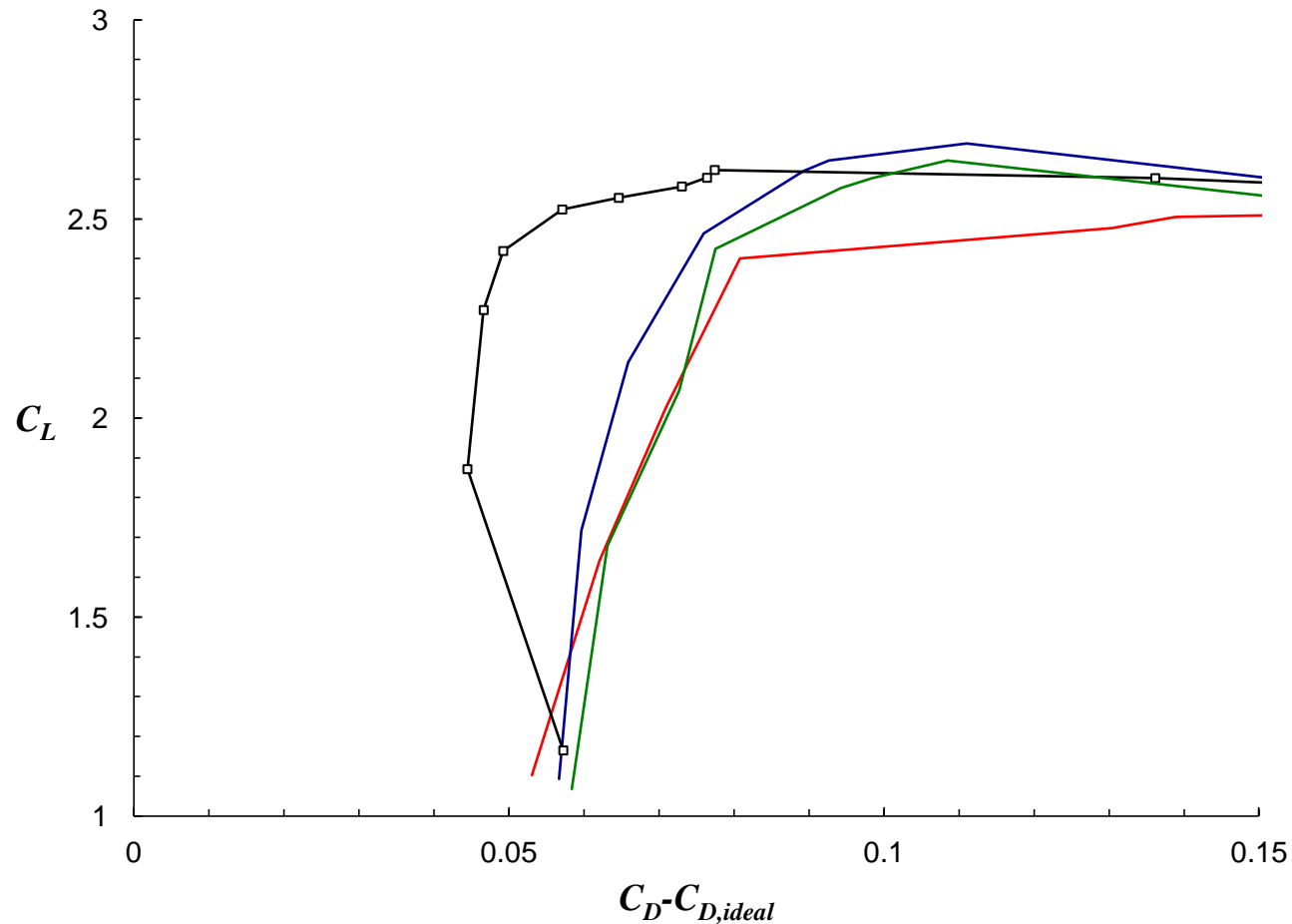
- Lift, SST-based models





# Comparison of Transition Models, $Re = 1.35 \times 10^6$

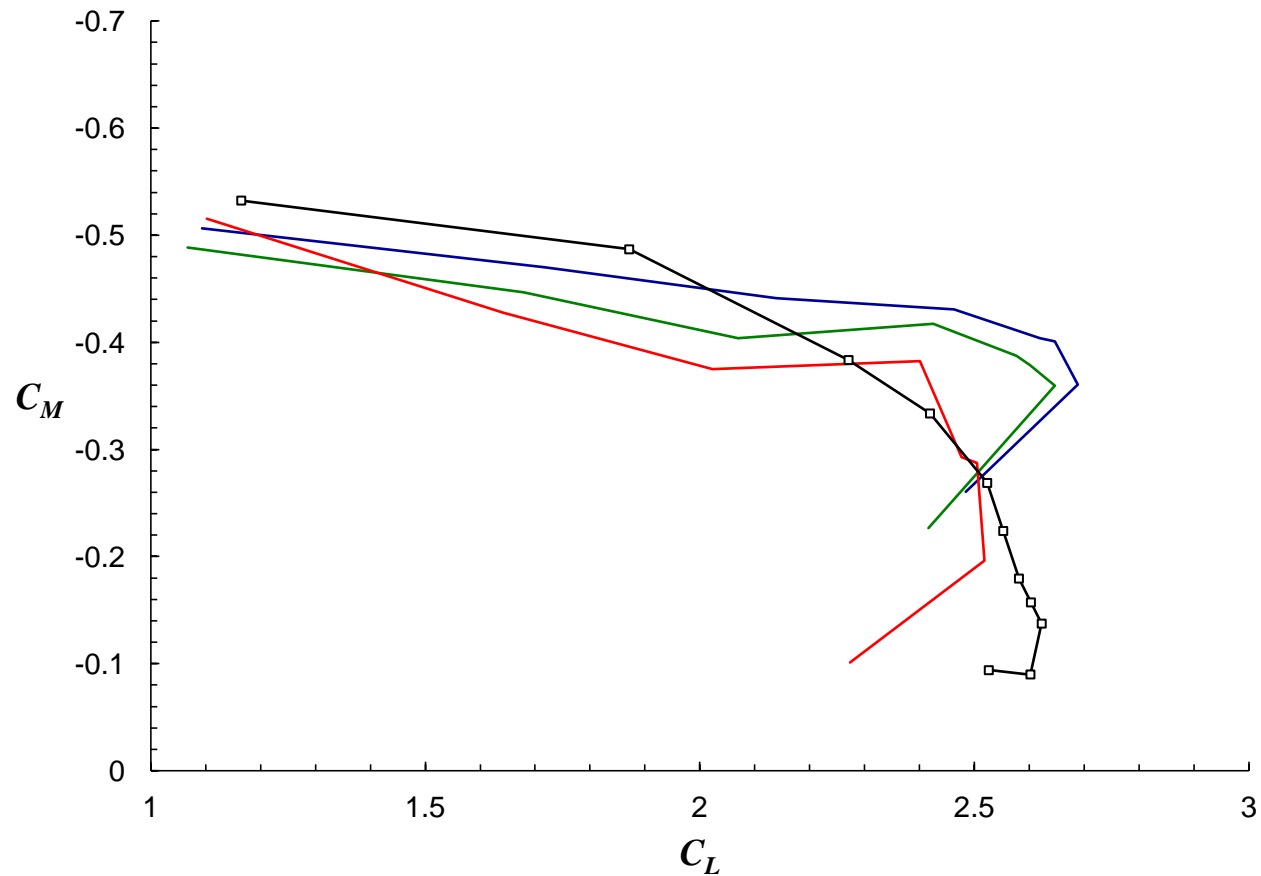
- “Profile” Drag, SST-based models





# Comparison of Transition Models, $Re = 1.35 \times 10^6$

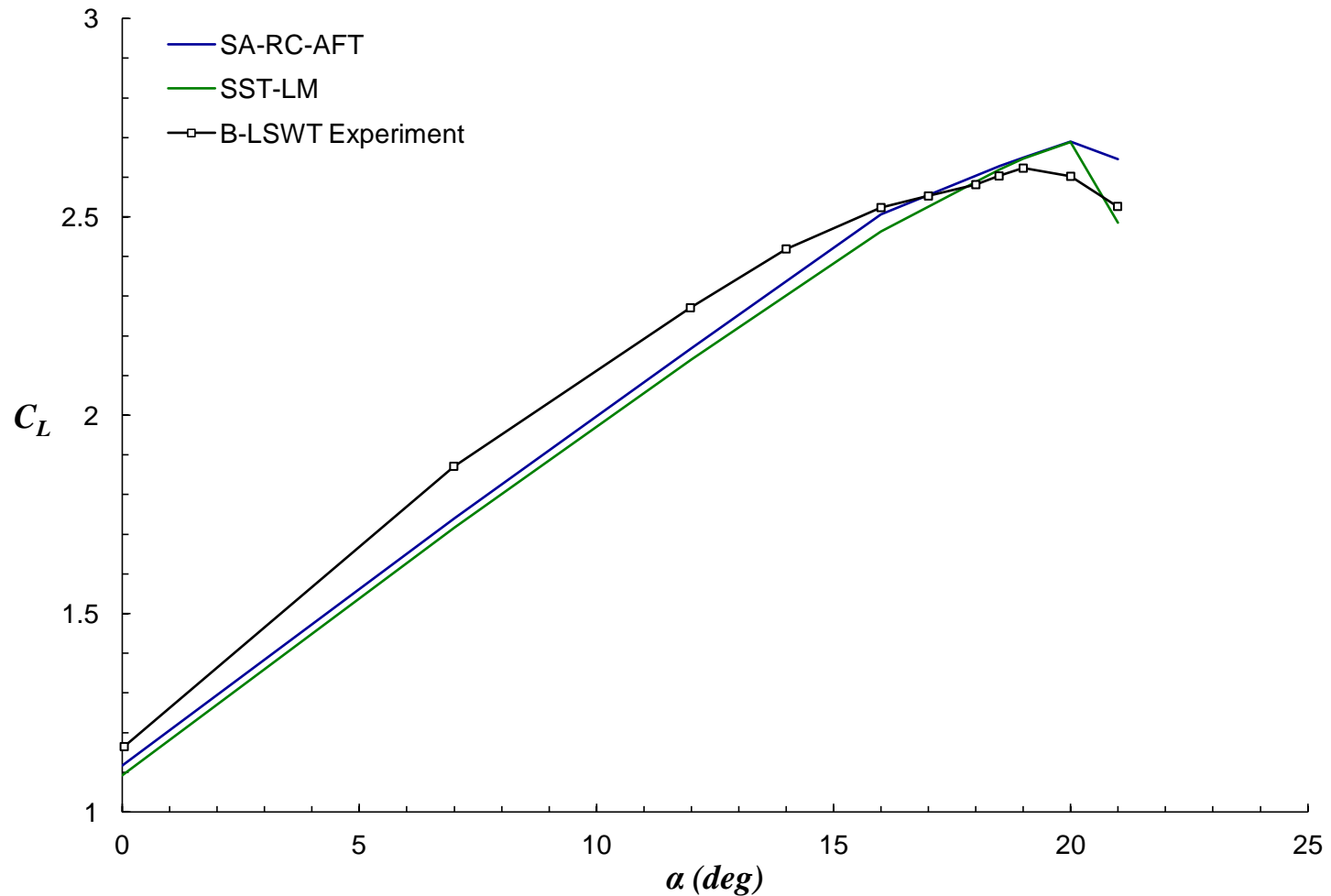
- Pitching Moment, SST-based models





## Comparison of Transition Models, $Re = 1.35 \times 10^6$

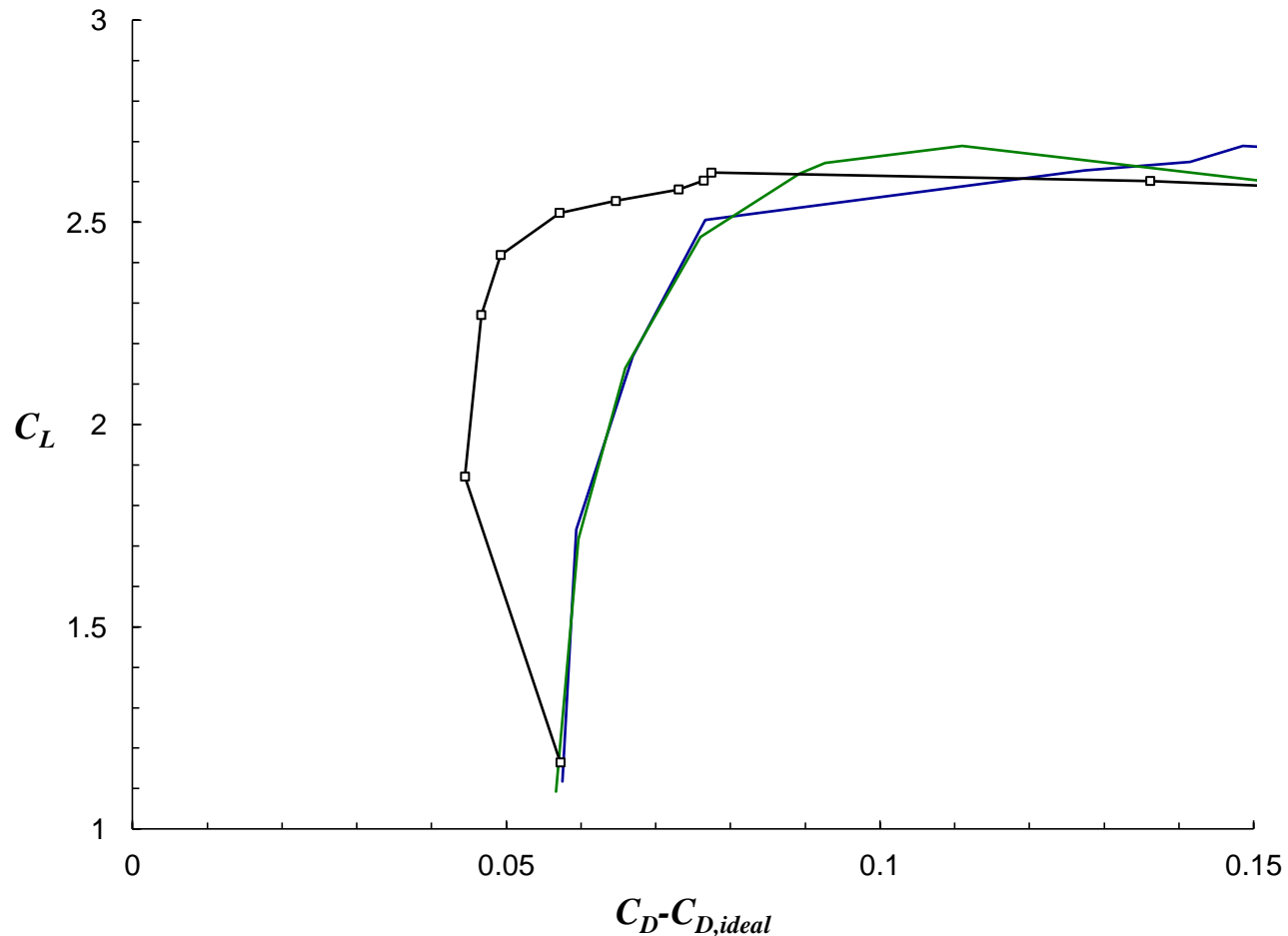
- Lift, similar results from different models





## Comparison of Transition Models, $Re = 1.35 \times 10^6$

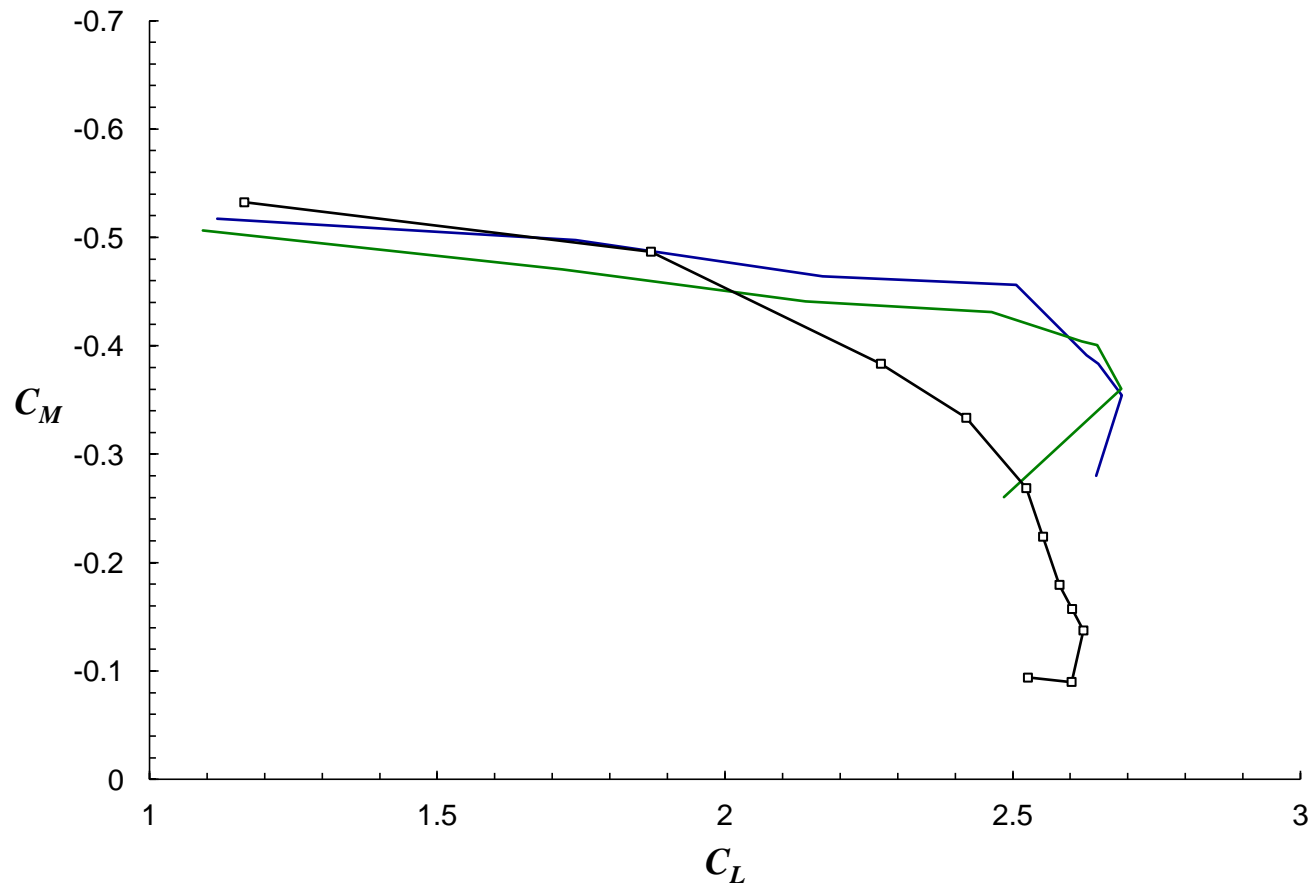
- “Profile” Drag, similar results from different models





## Comparison of Transition Models, $Re = 1.35 \times 10^6$

- Pitching Moment, similar results from different models

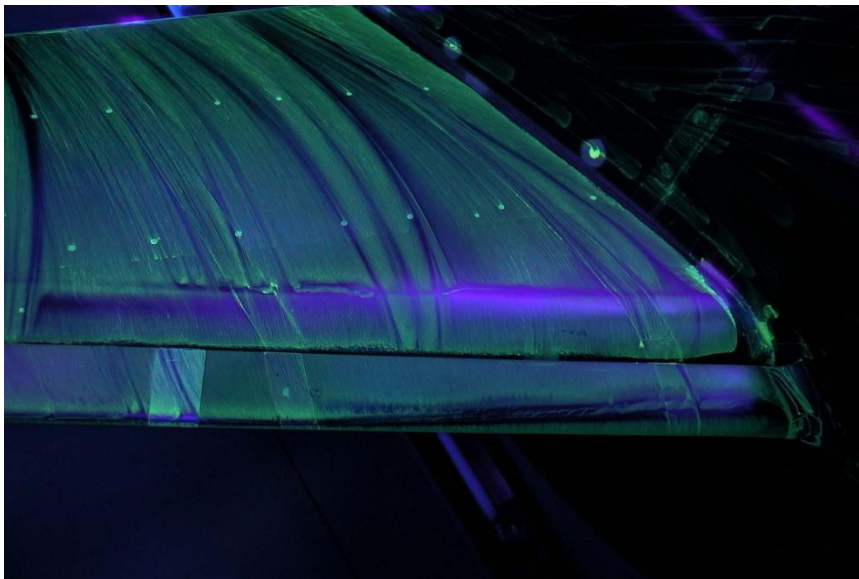




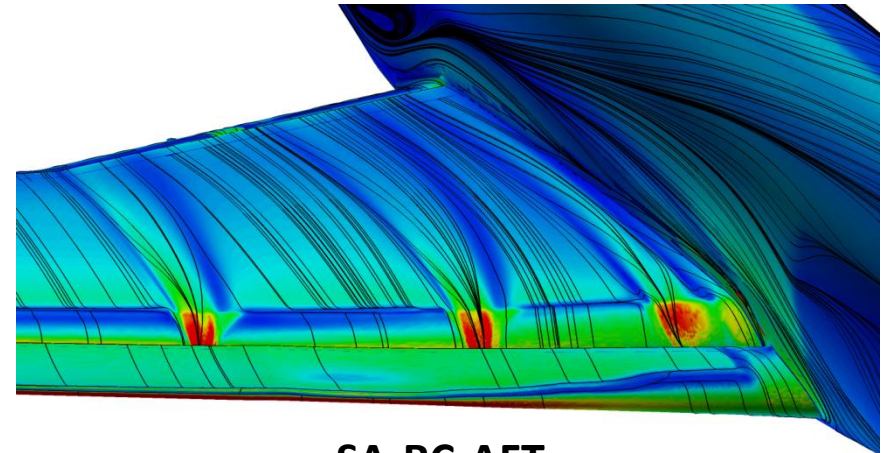
Case 2

Comparison of Transition Models,  $Re = 1.35 \times 10^6$

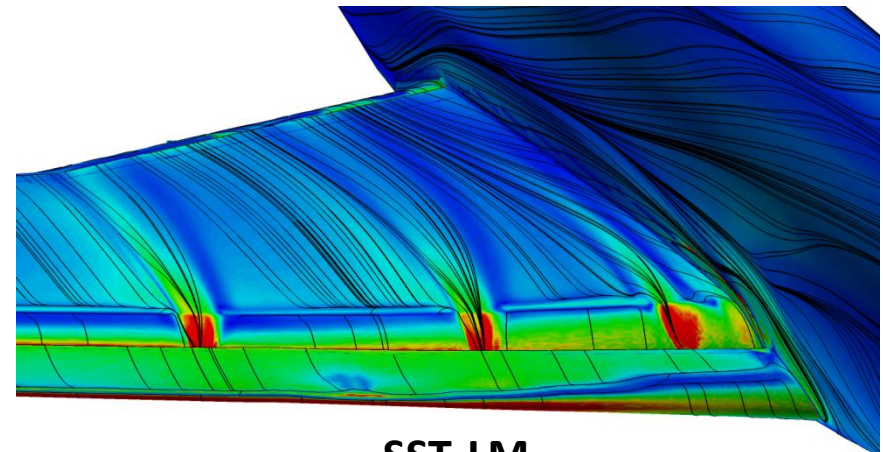
- Surface flow patterns,  $\alpha = 18.5^\circ$



Experiment



SA-RC-AFT



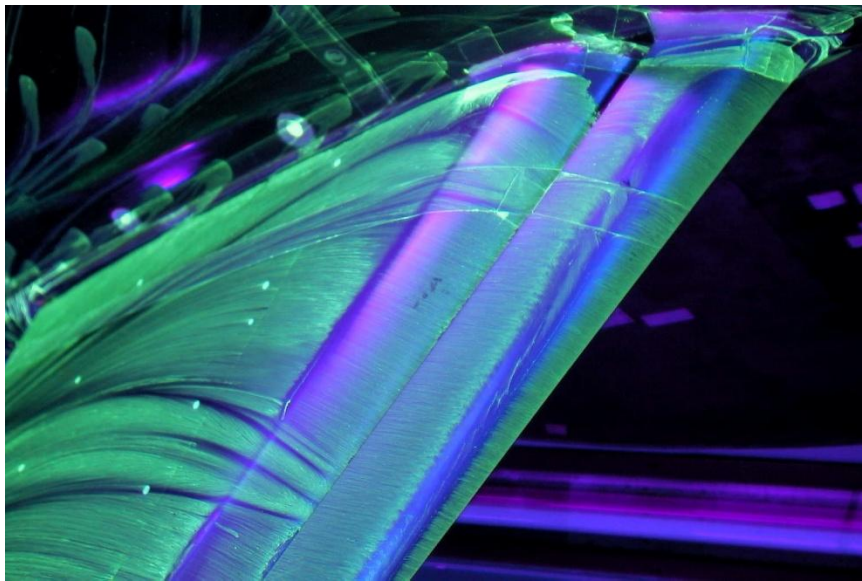
SST-LM



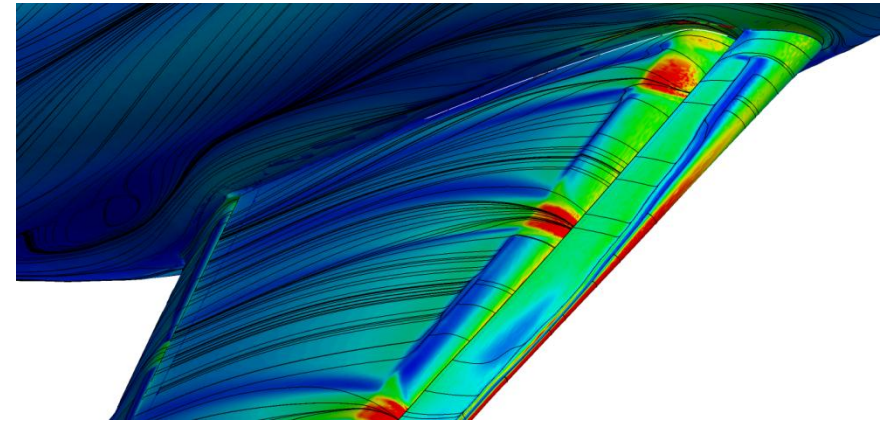
Case 2

Comparison of Transition Models,  $Re = 1.35 \times 10^6$

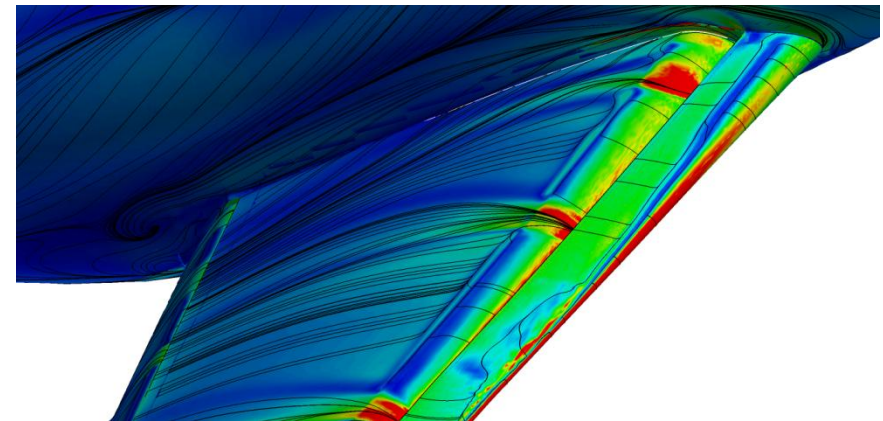
- Surface flow patterns,  $\alpha = 21^\circ$



Experiment



SA-RC-AFT



SST-LM



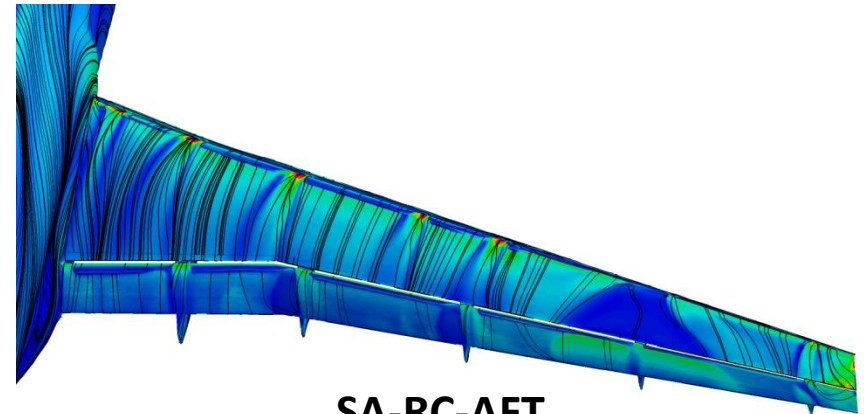
Case 2

Comparison of Transition Models,  $Re = 1.35 \times 10^6$

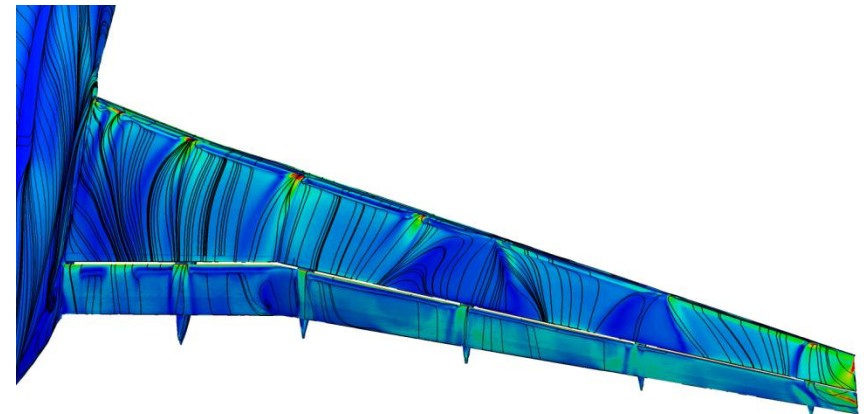
- Surface flow patterns,  $\alpha = 21^\circ$



Experiment



SA-RC-AFT



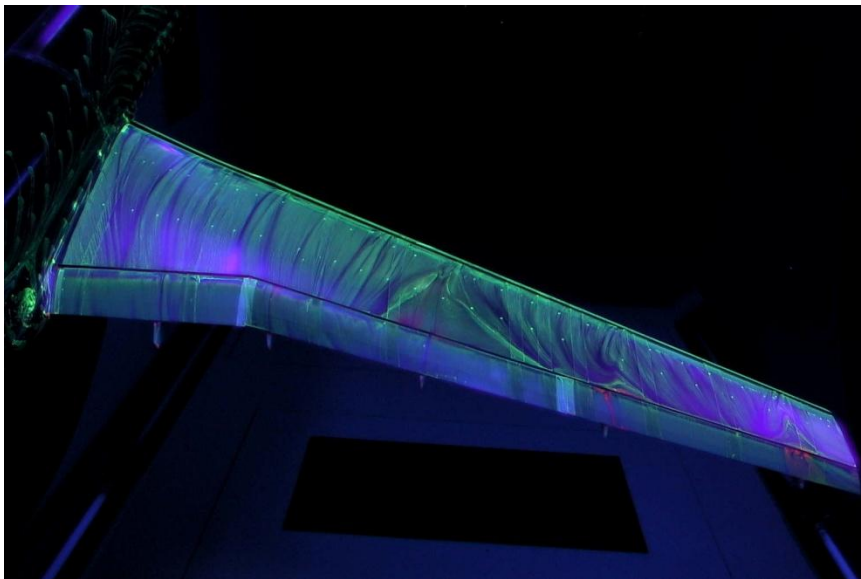
SST-LM



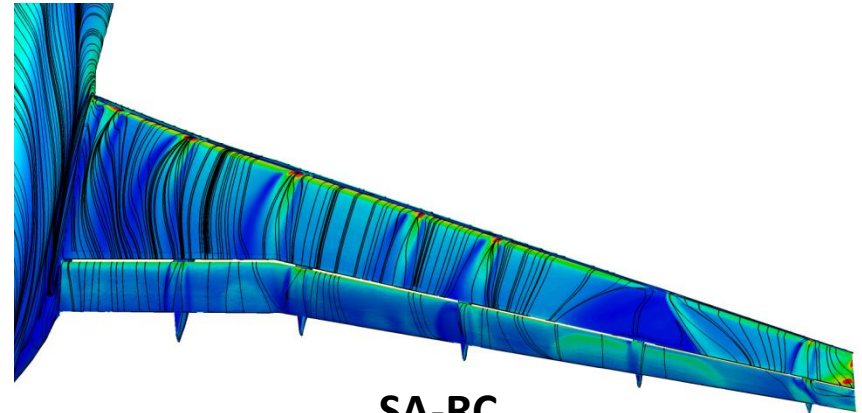
Case 2

Comparison of Transition Models,  $Re = 1.35 \times 10^6$

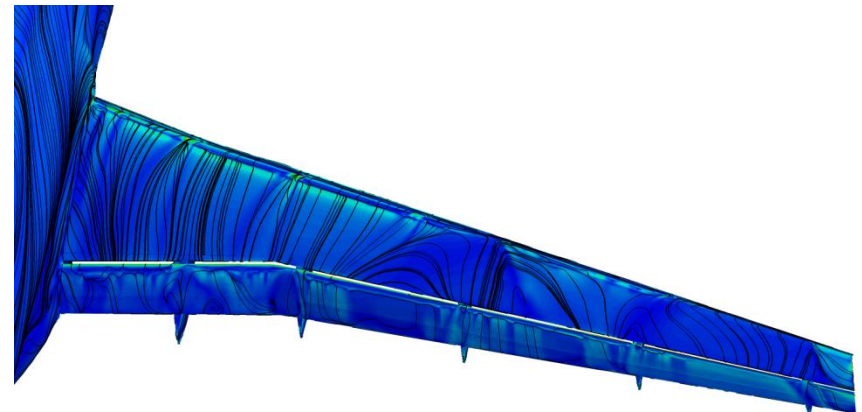
- Surface flow patterns,  $\alpha = 21^\circ$  - FULLY TURBULENT



Experiment



SA-RC



SST



## Outline

- Background and Motivation
- Geometry and Case Descriptions
- Solver, Methods, and Grids
- Turbulence and Transition Models
- Selected Results
  - Case 1 (Brackets off)
  - Case 2 (Brackets on)
- **Observations, Conclusions, and Future Work**



## Observations and Conclusions

- None of the turbulence model variants accurately predicted the aerodynamic characteristics of this high-lift configuration
  - Maximum lift dominated by viscous, trailing-edge stall
  - Effective zero-lift angle of attack discrepancies
  - Character of the drag polar not captured
- Very sensitive to geometric fidelity
  - Slat and flap brackets reduce suction peaks, change separation patterns
  - Shift in lift curve from Config. 2 to Config. 4 too much
- SST variants predicted the stall mechanism more accurately than SA
  - SA predicted the critical separation wedge to occur further outboard
- Transition did not have as big of an impact as expected!



## Future Work

- Analyze Config. 5 with same transition and turbulence modeling techniques
- Further investigate influence of low-Mach preconditioning
  - Configs. 4 and 5
  - Some other, relatively simple configuration?
- Apply the AFT transition model to the SST turbulence model for this geometry
  - Final testing of SST-AFT is underway
  - Abstract submitted for AIAA SciTech 2015



## Acknowledgments

- This research was conducted with government support under and awarded by the Department of Defense, High-Performance Computing Modernization Program, National Defense Science and Engineering Graduate Fellowship, 32 CFR 168a. All computational fluid dynamics cases presented in this paper were run on computer systems operated and maintained by Department of Defense High Performance Computing Modernization Program.
- The author also thanks Boeing Research and Technology, Huntington Beach, CA for supporting the original presentation of this research at the 2<sup>nd</sup> AIAA High-Lift Prediction Workshop, 22-23 June 2013, San Diego, CA.



**Thank you for your time**

